

# Particle Image Velocimetry Measurement in the Model of Vascular Anastomosis

**Grus T.<sup>1</sup>, Lindner J.<sup>1</sup>, Vik K.<sup>1</sup>, Tošovský J.<sup>1</sup>, Matěcha J.<sup>2</sup>,  
Netřebská H.<sup>2</sup>, Tůma J.<sup>2</sup>, Adamec J.<sup>2</sup>**

<sup>1</sup>Second Surgical Department – Clinical Department of Cardiovascular Surgery of the First Faculty of Medicine, Charles University in Prague, and General Teaching Hospital, Czech Republic;

<sup>2</sup>Department of Fluid Dynamics and Power Engineering, Czech Technical University in Prague, Czech Republic

Received January 26, 2007; Accepted February 14, 2007.

**Key words:** Neointimal hyperplasia – Vascular anastomosis – Particle image velocimetry – Wall shear stress – Flow pattern – 3D blood flow simulation – Computational fluid dynamics

*This research has been supported by grant of GA ČR 101/05/0675.*

**Mailing Address:** Tomáš Grus, MD., Second Surgical Department of Cardiovascular Surgery, U Nemocnice 2, 128 00 Prague 2, Czech Republic, e-mail: tgrus@seznam.cz

**Abstract:** Neointimal hyperplasia is the most common complication of all forms of arterial reconstructions. This response of the vascular wall to injury is influenced by many factors, especially, but not limited to, by the hemodynamic profile in the area of vascular anastomosis and in its close proximity. To eliminate this negative influence of hemodynamics on progression of neointimal hyperplasia, we tried to develop anastomosis with optimal hemodynamic parameters. In our experimental study we used Particle Image Velocimetry measurement and 3D blood flow simulation for studying flow characteristics for different length and angles of anastomoses. Based on our experimental studies and numerical simulations we believe that anastomosis with smaller angle demonstrates better hemodynamic parameters, optimal angle being less than 30 dg. Length of anastomosis in this smaller angle anastomosis is app. 2–2.5 of native vessel diameter.

## Introduction

Numerous bypass grafts are implanted annually worldwide to relieve coronary arterial obstruction. However, up to 25% of the grafts fail by the end of first year and up to 50% of the grafts fail by the end of first decade [1, 2]. The principal cause of graft failure is stenosis secondary to intimal hyperplasia. There is a well known relationship between vessel wall biology and the local flow parameters, with wall shear stress (WSS) being one of the most influential [3, 4, 5, 6, 7].

In spite of the fact that there is no definite opinion on how WSS values or WSS distribution influence the development of neointimal hyperplasia, it is generally assumed that these values and distribution should not differ from physiological ones.

The research of hemodynamics in the bypass connection is carried out both *in vivo* and *in vitro*. The *in vivo* studies present results from the experiments with laboratory animals [8], or present long-term patient follow-ups of restenosis or describe flow characteristics in anastomosis [9, 10]. The studies presenting *in vivo* measurements study the influence of geometry of anastomosis on flow characteristics (i.e. on WSS [10, 11, 12]), deal with the comparison of end-to-side and end-to-end anastomosis [13] or secondary flow in the distal part of bypass [14].

Several *in vitro* studies investigate the influence of hemodynamics on the progression of (vascular diseases). The effect of different characteristics such as angle of anastomosis [15, 16, 17], symmetry of anastomosis [18], shape of anastomosis [19], pulse shape and inlet velocity profile shape are being investigated. Authors correlate diseases with different flow characteristics by measuring with pressure magnitude, shear stress magnitude [18], turbulence intensity and flow rate ratio [21, 22].

*In vitro* hemodynamic flow velocity measurements have been performed using Laser Doppler Anemometry (LDA) [20, 24], Particle Image Velocimetry (PIV) [25] and Ultrasonic Velocity Profiling (UVP) [18, 26].

*In vitro* research is also being performed by numerical simulation, using computational fluid dynamics (CFD) or 3D blood flow simulation [27, 28, 29, 30, 31]. This new progressive CFD method of computation allows more precise approximation both to the reality and to the experiment and also allows to obtain information in parts of experimental model where it is difficult to insert the measurement probe or in case when obtaining complex information about the flow would increase the number of necessary measurements.

The objective of our long-term project is to find the optimal shape of the end-to-side anastomosis. The negative impact of flow dynamics on the vascular walls and blood can be minimized, therefore reducing the risk of bypass graft failure. This study is based on the results of our previous experiments *in vitro* we used the laser doppler anemometry (LDA) method to analyze unsteady flow [32] and particle image velocimetry (PIV) method for investigation of flow in cardiovascular models [14, 21]. The influence of the angle of end-to-side anastomosis on flow field characteristics was investigated in different flow rates both in native arteries and bypass grafts.

### Materials and Methods

The vessel anastomosis (Figure 1) for vessel diameter from  $d=4$  to 6 mm, blood kinematics viscosity  $\eta = 4.10^{-6} \text{ m}^2 \text{ s}^{-1}$  and flow rate from  $Q = 500 \text{ cm}^3 \text{ min}^{-1}$  to  $1000 \text{ cm}^3 \text{ min}^{-1}$  was modelled. The similitude theory used for blood flow model determines conditions when the fluid flow in anastomosis model is physically similar to blood flow in vessel anastomosis. The similitude dictates accord of dimensionless numbers. The Reynolds number ( $Re = vd/\eta$ ), where  $v$  is average velocity,  $d$  is diameter of tube and  $\eta$  is kinematics viscosity, is used in our case of stationary flow. The range of dimensionless Reynolds number is from  $Re = 500$  to 1400 for our case. The set of experimental and numerical models were created for these flow parameters. The models had graft and host artery diameter  $d = 10$  mm with different anastomosis angle ( $\alpha = 20^\circ, 30^\circ, 45^\circ, 60^\circ$  and  $90^\circ$ ).

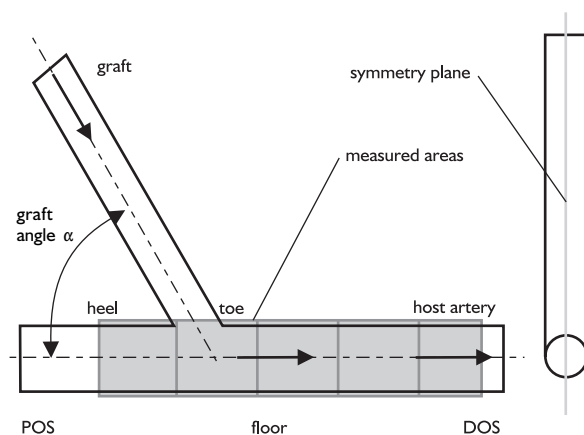


Figure 1 – Scheme of the bypass model for measurement by PIV method. In the picture the parts of bypass are illustrated: the symmetry plane where the PIV measurement was carried out, the measured areas, the areas of proximal outlet segment (POS) and distal outlet segment (DOS).

*Experimental equipment*

The experimental equipment (Figure 2) for visualization and measurement by PIV method in symmetry plane of bypass junction for steady conditions was made. The liquid was pumped into a tank with overflow to create a constant pressure gradient. The liquid passed from the tank through the first ultrasound flow meter and through a valve, which could change total flow rate. Fluid then continued into the tube simulating the native artery and then into the model of bypass anastomosis. The second ultrasound flow meter and valve were placed in the tube simulating the bypass graft and it allowed a controlled flow rate between native artery and graft and to simulate different rate of stenosis.

*Visualization*

The glass models were made for visualization. Water was used as a working fluid. The silver covered glass sphere particles (S-HGS  $10\mu\text{m}$ ) were added into water as seeding particles. These were illuminated with red laser diode with wave length 650 nm. The beam was conducted through the cylindrical lens which created the light sheet. Particles added into fluid were scanned by camera Lumenera Lu175 (Frame Rate 15 fps at  $1280\times 1024$ , 60 fps at  $640\times 480$ ). Visualization was carried out for flow regimes corresponding with Re 500 and 1 400 in symmetry plane and in parallel planes.

*PIV measurement*

The principle of PIV method is measuring the movement of the particles, which are added to the working fluid, during the known time interval. The PIV system

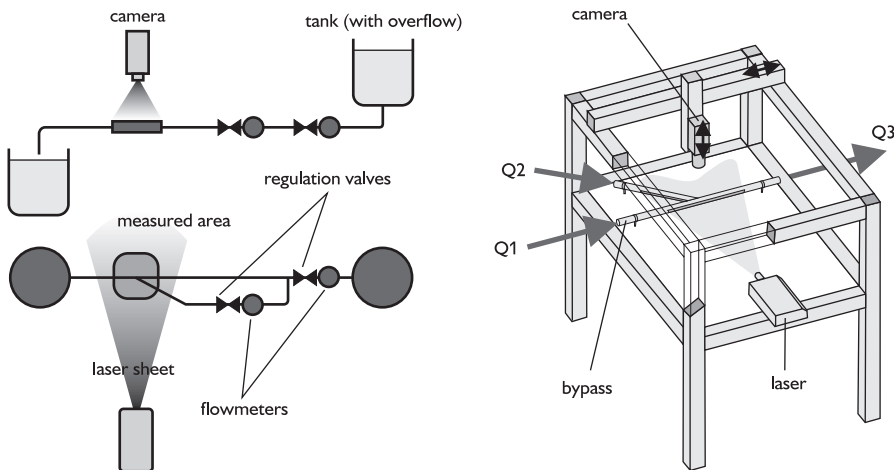


Figure 2 – Left: Experimental equipment for visualization and flow fields measurement by PIV. Right: Scheme of measuring place with fixed model.  $Q_1$ ,  $Q_2$ ,  $Q_3$  are flow rates in different parts of the model. Laser and camera are placed on the sliding equipments, which enabled illumination and taking photos of precisely determined place.

from Dantec Dynamics which comprises these components: a pair of cameras Dantec HiSense, 1 024k × 1 280k pixel CCD, frequency 4.5 Hz for double frame mode and 9 Hz for single frame mode; a pair of pulsed lasers Nd:YAG New Wave Gemini 15 Hz–120 mJ, with optics; PIV processor Dantec FlowMap 1500, 2 × 1 Gb buffer was used.

The bypass models were made from plexiglas for PIV measurements. Solution of sodium-iodine (58% NaI,  $\rho = 1730 \text{ kg/m}^3$ ,  $\eta = 0,00254 \text{ Ns/m}^2$ ,  $t = 24^\circ\text{C}$ ) was used as a working fluid. NaI solution was used because its refractive index is the same as the refractive index of plexiglas and thus the optical distortions between model and working fluid were minimized. Fluorescent particles with diameter 1–20  $\mu\text{m}$  were used as seeding particles. This type of particles was used because it allows filtering reflexes from laser in the boundary of model and liquid. If these particles are illuminated with ND-YAG laser ( $\lambda = 532 \text{ nm}$ ) and if the screen for the camera (which transmits only the light with the wave length higher than  $\lambda = 580 \text{ nm}$ ) is used then it is possible to scan only the light emitted from the particles and thus to filter out the reflections.

The flow field was measured in symmetry plane of the model for steady conditions ( $Re = 500; 1400$ ). Six areas (Figure 1) were measured along the native artery (length of measured area was approximately 60 mm). The instantaneous velocity fields and time-averaged velocity fields with velocity fluctuations were evaluated. The velocity gradients near the wall were evaluated [33]. These gradients multiplied with working fluid dynamic viscosity correspond with wall shear stress. The post processing in PIV measurement is very important. Using correct post processing enables removal of signal noise from the background and reflection generated by wall and thus increases the accuracy of measurement [34, 35].

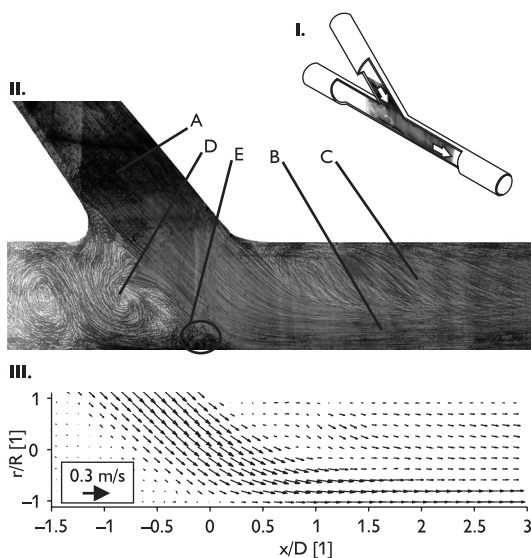


Figure 3 – The flow field in symmetry plane. I. Scheme of flow in anastomosis. II. Result of visualization in the symmetry plane: A) incoming flow, B) flow in the symmetry plane accelerates in connection place and continues around floor, C) secondary flow, D) vortex structure, E) area with intensive velocity gradient, which is moving parallel to the host artery axis. III. PIV visualization of model for  $45^\circ$  by-pass connection angle and  $Re = 1400$ . The arrows illustrate velocity in every point. Direction of flow is illustrated by direction of arrows and velocity of flow is illustrated by size of arrows. Distance in host artery direction, which is multiplied by the diameter of host artery, is on the horizontal axis. Distance from host artery centre, which is multiplied by the host artery radius, is on the vertical axis.

*Numerical simulation*

Numerical simulations were carried out for the same models as experiments. They consist of two tubes with inner diameter  $d = 10$  mm. The length of graft to junction was  $l = 700$  mm. The length of proximal outlet segment (POS) was 100 mm and it was closed in order to simulate the stenosis. The length of distal outlet segment (DOS) was  $l = 700$  mm. 3D computation grid was generated with hexahedron elements of about 800 000 cells. Numerical solutions were carried out for the same conditions as experiments (working fluid, flow rate in native artery and graft). The mathematical model was selected as the laminar model. The boundary conditions were set on the input to the graft – velocity inlet, on input to the native artery – wall and on the output – pressure outlet.

**Results**

The complex space flow was built in an anastomosis model. Numerical and experimental models were shaped so that the developed laminar velocity profile could be entered at the anastomotic region. The flow stream coming from graft begins to form helix vortex structures after entering the anastomosis (Figure 4).

The symmetry plane visualization demonstrates that the inlet flow (Figure 3A) (only flow lines in symmetry plane) in the symmetry plane gets to the floor and then the flow accelerates and goes parallel with x axis as a narrow jet (Figure 3B). There is also a very distinct area opposite to the floor (Figure 3C) with a secondary flow.

The character of complex vortex structures created in the POS area depends on the liquid flow parameters. They look like two vortices in the symmetry plane (Figure 3E). The shape of these vortices is strongly dependent on the stenosis distance from the anastomosis. The flow outside the symmetry plane moves in the form of a helical shaped vortex structure with variable spiral angle.

Vortex structures are shown in figure 3. These structures create secondary flow in the cross section. The secondary flow intensity decreases downstream and the velocity profile is gradually formed into developed laminar velocity profile. There is an area with strong velocity gradient (Figure 3E) between the main flow (Figure 3B) and the vortex structure in POS area (Figure 3D). The size and placing of this area is time-dependent both by steady and unsteady inlet conditions. In this area the magnitude of WSS is maximal due to the large velocity gradients. Maximum WSS is time-dependent and shifts along the x axis downstream and upstream that causes wall shear stress oscillation. Future investigation will be focused on this area.

The comparison of visualization with PIV results was carried out. Figure 3 shows that flow field evaluated from PIV measurement correlates with the flow shape demonstrated by direct visualization.

Comparatively good correlation between the experiments and numeric simulations of flow in bypass was shown on velocity profile characteristics

(Figures 5 and 6). The deviation of these profiles in symmetry plane can be caused by several causes.

### Discussion

The velocity in the bypass was derived from measured mass flow data. Because of ultrasound meter accuracy some differences existed between real and measured data.

Laser sheet has non-zero thickness and therefore CCD camera records signal from seeding particles which are not in symmetry plane only. It can cause inaccuracy of measured data.

Selected laminar computational model was a source of inaccuracy because the definition of type of flow in the place behind the connection is different due to the secondary flow.

Many models would have to be constructed and each model would have to be checked in a large number of measurements in order to find out the optimal bypass junction shape with the help of an experimental research only. Due to good agreement of numerical and experimental results it was possible to decrease the

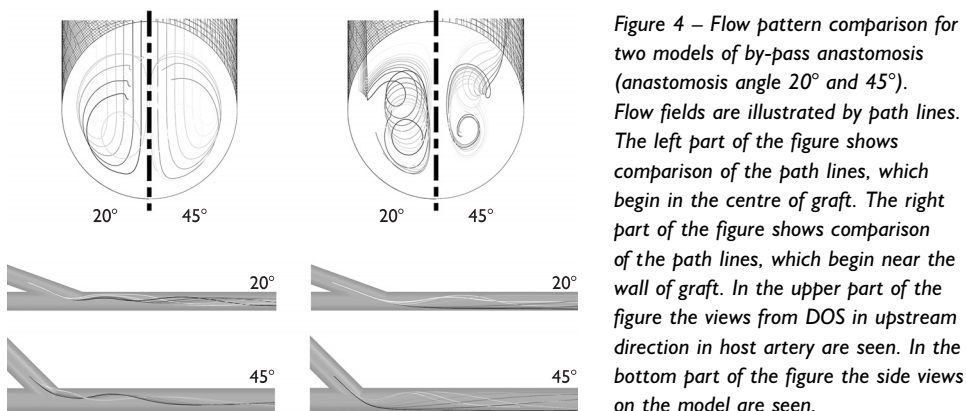


Figure 4 – Flow pattern comparison for two models of by-pass anastomosis (anastomosis angle 20° and 45°). Flow fields are illustrated by path lines. The left part of the figure shows comparison of the path lines, which begin in the centre of graft. The right part of the figure shows comparison of the path lines, which begin near the wall of graft. In the upper part of the figure the views from DOS in upstream direction in host artery are seen. In the bottom part of the figure the side views on the model are seen.

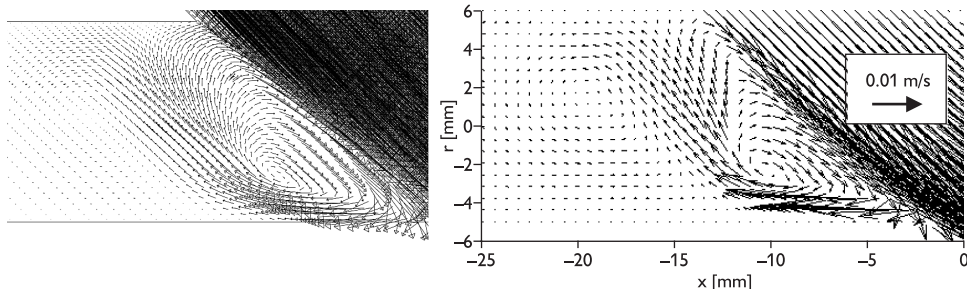


Figure 5 – Vortex structure in symmetry plane model in POS area with connection angle 45° and  $Re=1400$ . Left: numerical simulation, Right: PIV experimental measurement. A good quality and quantity agreement between numerical and experimental solution is visible.

number of experiments planned to do in future only to necessary amount and replace these experiments with numerical simulation.

The influence of the graft angle on flow field is seen in figure 6 and 7. They show the velocity fields in symmetry plane measured by PIV. The secondary flow intensity increases with increasing anastomosis angle. In the region in host artery (Figure 7) the flow field in the host artery axis direction has monotonic decreasing character for the small graft angle. The areas with higher and lower velocity appear in this region with increasing angle at the projection of flow field into symmetry plane. It is caused by increasing secondary flow with increasing graft angle which can be seen from the numerical simulation.

The space distributions of WSS evaluated from CFD are shown in figure 8 – right. The magnitude of WSS behind the graft junction rises. Maximum value of WSS is in the floor region.

The behaviors of WSS evaluated from CFD in symmetry plane for floor line for different graft angles are shown in figure 8 – left. Maximum value of WSS is approximately in distance of one diameter from the junction. It shifts downstream for bigger graft angles and upstream for smaller graft angles. The maximum value of WSS rises with rising graft angle. The WSS drop to value close to WSS value during developed laminar flow is faster for smaller angles than for bigger angles. The character of the behavior of WSS is similar for floor and opposite the floor of anastomosis. For floor of the anastomosis, maximum values are approximately three to four times bigger.

The values of velocity profile gradient on the floor, multiplied with dynamic viscosity of working fluid, were evaluated from PIV data for several models and

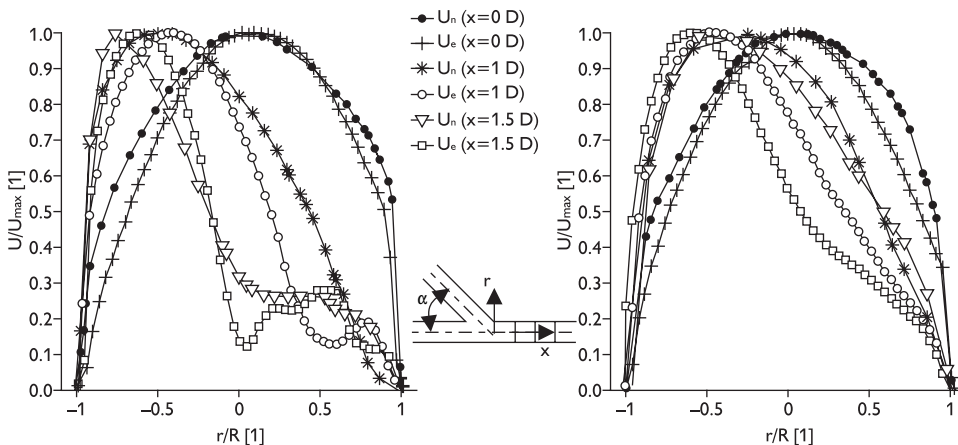


Figure 6 – Comparison of experimental (marked with subscript e) and numerical (marked with subscript n) velocity profiles in cross sections  $x = 0; 1; 1.5 D$ . Left: for angle  $\alpha = 45^\circ$ . Right: for angle  $\alpha = 20^\circ$ . In the pictures we can see a good agreement between numerical and experimental solution. Comparison of the flow fields shows that the region of secondary flow is bigger for angle connection  $\alpha = 45^\circ$ .

several measured regimes. The character of behavior of these values is similar to WSS evaluated from CFD. The maximum value of WSS increases with increasing flow rate. In case that flow rate in graft is 75% of the total flow rate then the maximum values of WSS decrease.

The pathological phenomenons in the anastomosis are induced by many factors. Some of them are studied by hemodynamics. The shear stress in blood flow stream is assuredly one of the parameters that influence interactive impingement of fluid flow most, causing blood corpuscles to dash against vessel wall and their damage. These reasons lead us to deal with WSS thoroughly and therefore it was chosen as optimization parameter when solving the bypass.

The blood is non-Newtonian fluid with complicated thermophysical properties, the mechanical vessel properties are difficult to describe and the flow quantities are time dependent. This is the reason why the first phase of hemodynamics research of cardiovascular system parts proceeds on simplified models. This relates both for mathematical and experimental models carried out *in vitro*. It is generally possible to determine WSS experimentally by two ways:

- indirectly – evaluation of measured velocity profile,
- directly – with the help of special probe (CTA).

The velocity field determination has crucial meaning for finding hemodynamics parameters and thus WSS. The measured velocity profiles allow evaluating WSS. We prefer non-invasive methods for velocity field measurement because they do not influence the flow. These methods are used most often for this sort of measurement:

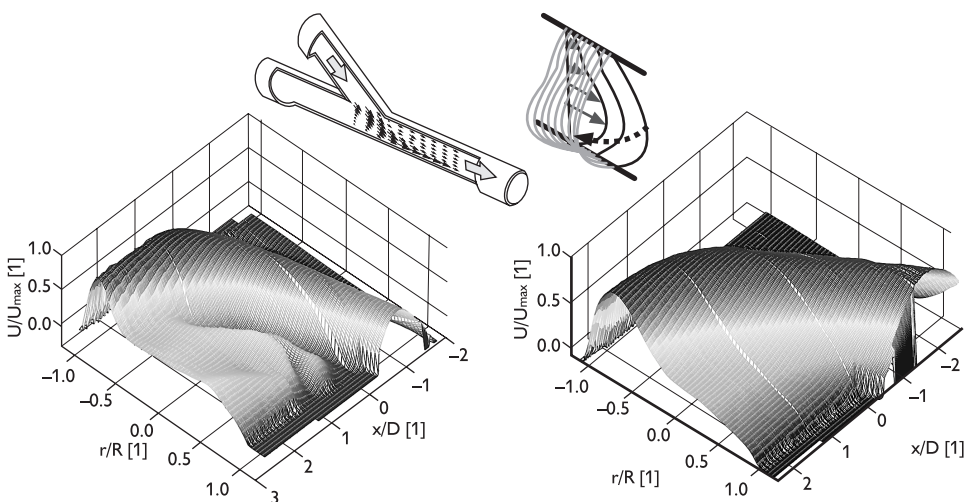


Figure 7 – Velocity distribution in  $x$  direction for  $Re$  1400 from PIV. Velocity in direction  $x$  is projected to the  $z$ -axis, as it is illustrated in the small pictures. Left: velocity fields in direction  $x$  for connection angle  $45^\circ$ . Right: velocity fields in direction  $x$  for connection angle  $20^\circ$ .

- Ultrasonic Velocity Profiling (UVP),
- Laser-Doppler Anemometry (LDA),
- Particle Image Velocimetry (PIV).

When using UVP method we measure velocity with the help of ultrasound. LDA and PIV belong to the optical methods. These methods measure velocity of particles added into the working fluid in model.

When we compare the methods mentioned above the PIV method appears to be the most suitable. It is the most modern method with enormous progress possibility. It does not disturb the flow and allows measuring instantaneous velocity field (in requested plane) on the instant. It also allows evaluating mean velocity and fluctuation deviations. PIV has the advantage in comparison with LDA and UVP due to the fact that PIV measures the velocity field on the instant and LDA measures velocity point by point and UVP method measures velocity in one line. The WSS evaluation based on velocity profile uses instantaneous velocity field and no velocity profile which is measured point by point. The PIV method is the most precise and the least time-consuming method which results from the reasons mentioned above.

The models used in experiments are designed in conformity with physical similitude laws and they must satisfy the specific conditions of measurement method. In case of PIV method the models must be transparent and model material and working fluid must have certain optical properties.

We realize that graft patency is influenced by many factors, but we consider angle of anastomosis to be one of the most important and in real life of those the most easily changed. Based on our results we believe, that endorsing parameters

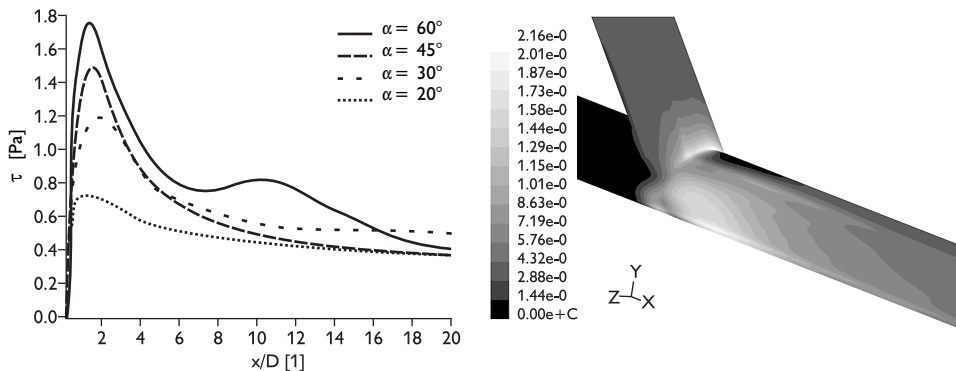


Figure 8 – Wall shear stress computed by numerical simulation. Left: Comparison of WSS on the floor for different angles from numerical simulation. The areas of shear stress maximum are in the distance  $x/D$  is 1 to 2. In these areas the post operation complications are very frequent. Right: Wall shear stress for angle  $45^\circ$  from numerical simulation. The gray scale represents the quantity of wall shear stress. The areas of higher shear stress values are illustrated in the figure. The shear stress values correspond with flow field obtained by PIV measurement.

of anastomosis mentioned above, i.e. small angle of anastomosis and appropriate length of anastomosis, gives us a chance of higher long-term patency of vascular anastomosis. The reason is that the anastomosis of smaller angle has lower maximum value of shear stress, lower secondary flow and lower velocity fluctuation. Length of anastomosis in this smaller angle anastomosis is app. 2–2.5 of native vessel diameter.

## References

1. BRYAN A. J., ANGELINI G. D.: The biology of saphenous vein graft occlusion: etiology and strategies for prevention. *Current Opinion in Cardiology* 9: 641–649, 1994.
2. CHESHIRE N. J., WOLFE J. H.: Infrainguinal graft surveillance: a biased overview. *Seminars in Vascular Surgery* 6: 143–149, 1993.
3. DAVIES P.: Flow-mediated endothelial mechanotransduction. *Physiol. Rev.* 75: 519–560, 1995.
4. HARUGUCHI H., TERAOKA S.: Intimal hyperplasia and hemodynamic factors in arterial bypass and arteriovenous grafts: a review. *Japan. Soc. for Artificial Organs* 6: 227–235, 2003.
5. BASSIOUNY H. S., WHITE S., GLAGOV S., CHOI E., GIDDENS D. P., ZARINS C. K.: Anastomotic intimal hyperplasia: mechanical injury or flow induced. *J. Surgery* 15: 708–717, 1992.
6. BERGUER R., HIGGINS R. F., REDDY D. J.: Intimal hyperplasia. An experimental study. *Archives of Surg.* 115: 332–335, 1980.
7. KEYNTON R. S., EVANCHO M. M., SIMS R. L., RODWAY N. V., GOBIN A., RITTGERS S. E.: Intimal hyperplasia and wall shear in arterial bypass graft distal anastomoses: an *in vivo* model study. *J. Biomechanical Eng.* 123: 464–473, 2001.
8. TOZZI P., SOLEM J. O., BOUMZEBRA D., MUCCIOLO A., GENTON C. Y., CHAUBERT P., SEGESSER L. K.: Is the GraftConnector a Valid Alternative to Running Suture in End-to-Side Coronary Arteries Anastomoses? *The Society of Thoracic Surgeon* 72: 999–1003, 2001.
9. GREENWALD S. E., BERRY C. L.: Improving vascular grafts: the importance of mechanical and hemodynamic properties. *J. Pathology* 190: 292–299, 2000.
10. HOBALLAH J. J., MOHAN C. R., CHALMERS R. T. A., SCHUEPPERT M. T., SHARP W. J., KRESOWIK T. F., CORSON J. D.: Does the geometry of distal vein graft anastomosis affect patency? *Vascular Surg.* 30: 371–378, 1996.
11. OJHA M., COBBOLD R. S., JOHNSTON K. W.: Influence of angle on wall shear stress distribution for an end-to-side anastomosis. *J. Vascular Surg.* 19: 1067–1073, 1994.
12. ETHIER C. R., STEINMAN D. A., ZHANG X., KARPIK S. R., OJHA M.: Flow waveform effects on end-to-side anastomotic flow patterns. *J. Biomechanics* 31: 609–617, 1998.
13. HOEDT M. T., URK H., HOP W. C., LUGT A., WITTENS C. H.: A comparison of distal end-to-side and end-to-end anastomoses in femoropopliteal bypasses. *Euro. J. Vasc. and Endovasc. Surg.* 21: 266–270, 2001.
14. ANAYIOTOS A. S., PEDROSO P. D., ELEFThERIOU E. C., VENUGOPALAN R., HOLMAN W. L.: Effect of a flow-streamlining implant at the distal anastomosis of a coronary bypass graft. *Annals Biomed. Engineering* 30: 917–926, 2002.
15. JACKSON Z. S., ISHIBASHI H., GOTLIEB A. I., LANGILLE B. L.: Effects of anastomotic angle on vascular tissue responses at end-to-side arterial grafts. *J. Vascular Surg.* 34: 300–307, 2001.
16. LEE D., SU J. M., LIANG H. Y.: A numerical simulation of steady flow fields in a bypass tube. *J. Biomech.* 34: 1407–1416, 2001.
17. CHUA L. P., YU S. C. M., TAM W. P.: PIV measurements of proximal models with different anastomotic angles. *Int. Comm. in Heat and Mass Transf.* 27: 517–526, 2000.

18. SIOUFFI M., DEPLANO V., PÉLISSIER R.: Experimental analysis of unsteady flows through a stenosis. *J. Biomech.* 31: 11–19, 1998.
19. KHUNATORN Y., MAHALINGAM S., DEGROFF C. G., SHANDAS R.: Influence of connection geometry and SVC-IVC flow rate ratio on flow structures within the total cavopulmonary connection: A numerical study. *J. Biomech. Engineering* 124: 364–377, 2002.
20. LOTH F., JONES S. A., ZARINS CH. K., GIDDENS D. P., NASSAR R. F., GLAGOV S., BASSIOUNY H, S.: Relative contribution next term of wall shear stress and injury in experimental intimal thickening at PTFE end-to-side arterial anastomoses. *J. Biomech. Engineering* 124: 44–49, 2002.
21. LI X. M., RITTGERS S. E.: Hemodynamics factors at the distal end-to-side anastomosis of a bypass graft with different POS:DOS flow ratios. *J. Biomech. Engineering* 123: 270–276, 2001.
22. HUGHES P. E., HOW T. V.: Flow structures at the proximal side-to-end anastomosis influence of geometry and flow division. *J. Biomech. Engineering – transactions of the ASME* 117: 224–236, 1995.
23. CHENG CH. P., PARKER D., TAILOR, CH. A.: Wall shear stress quantification from magnetic resonance imaging data using lagrangian interpolation functions. Bioengineering Conference ASME, 2001, 50.
24. SIVANESAN S., HOW T. V., BLACK R. A., BAKRAN A.: Flow patterns in the radiocephalic arteriovenous fistula: next term an *in vitro* study. *J. of Biomechanics* 32: 915–925, 1999.
25. KNAPP Y. E., MOUREK B. F.: 2D-PIV measurements of the pulsative flow in a left heart simulator. Proceedings of PSFVIP-4, F4082: 1–9, France, 2003.
26. GAUPP S., WANG Y., HOW T. V., FISH P. J.: Characterisation of vortex shedding in vascular anastomosis models using pulsed doppler ultrasound. *J. of Biomech.* 32: 639–645, 1999.
27. COLE J. S., WATTERSON J. K., O'REILLY M. J. G.: Is there a haemodynamic advantage associated with cuffed arterial anastomoses? *J. of Biomech.* 35: 1337–1346, 2002 .
28. WALSH M. T., KAVANAGH E. G., O'BRIEN T., GRACE P. A., MCGLOUGHLIN T.: On the Existence of an Optimum End-to-side Junctional Geometry in Peripheral Bypass Surgery—A Computer Generated Study. *Eur. J. Vasc. and Endovasc. Surg.* 26: 649–656, 2003.
29. LONGEST P. W., KLEINSTREUER C., ARCHIE J. P.: Particle hemodynamics analysis of Miller cuff arterial anastomosis. *J. of Vasc. Surg.* 38: 1353–1362, 2003.
30. PAPAHRILAOU Y., DOORLY D. J., SHERWIN, S. J.: The influence of out-of-plane geometry on pulsatile flow within a distal end-to-side anastomosis. *J. of Biomech.* 35: 1225–1239, 2002.
31. BERTOLOTTI C., DEPLANO V.: Three-dimensional numerical simulations of flow through a stenosed coronary bypass. *J. of Biomech.* 33: 1011–1022, 2000.
32. ADAMEC J, NOŽIČKA J, HANUS D., KOŘENÁŘ J.: Experimental Investigation of Pulsatile Flow in Circular Tubes. *J. of Propulsion and Power* 17: 1133–1136, 2001.
33. MATĚCHA J., NETŘEBSKÁ H., TŮMA J., ADAMEC J, BÍCA M.: Flow Investigation behind the End-to-Side Anastomosis. The 16-th International Symposium on Transport Phenomena, Prague, 2005, 107.
34. NOVOTNÝ J.: Accuracy of Stereo PIV Measurement. 2nd International PhD Conference on Mechanical Engineering. Pilsen, 2004, 91–92.
35. PĚTA M., NOVOTNÝ J.: Image Processing in PIV The 16th International Symposium on Transport Phenomena. Prague, 2005, 40.